Kinetics of CO Substitution in $Co_4(CO)_{12}$ and $Rh_4(CO)_{12}$

J. RORY KENNEDY, FRED BASOLO*

Department of Chemistry, Northwestern University, Evanston, Ill. 60201, U.S.A.

and WILLIAM C. TROGLER*

Department of Chemistry, University of California at San Diego, La Jolla, Calif. 92093, U.S.A.

(Received September 16, 1987)

Abstract

The kinetics of rapid CO substitution by PPh_3 in $Co_4(CO)_{12}$ and $Rh_4(CO)_{12}$ have been examined by stopped-flow and low temperature FT-IR methods. In $Co_4(CO)_{12}$ rapid ($k_{obs} \sim 1.8$ s^{-1}) substitution of CO occurs after a 1–15 s induction period at 28 °C in C_6H_5Cl solvent by a catalytic process. Addition of PPh_3 to $Rh_4(CO)_{12}$ yields $Rh_4(CO)_{11}(PPh_3)$ according to a predominantly second order rate law $k_1[Rh_4(CO)_{12}] + k_2[Rh_4(CO)_{12}][PPh_3]$ with $k_1 = 25 \pm 11$ s^{-1} and $k_2 = 2.97 \pm 0.27 \times 10^4$ M^{-1} s^{-1} at 28 °C. Substitution of a second CO ligand also occurs rapidly with $k_1 = 0.15 \pm 0.09$ s^{-1} and $k_2 = 6.54 \pm 0.07 \times 10^2$ M^{-1} s^{-1} at 28 °C. The reactivity of $Rh_4(CO)_{12}$ toward associative substitution is 10^4–10^{11} faster than for the Co and Ir analogues. In $Rh_4(CO)_{11}(PPh_3)$ the increase in CO substitution rates over Co and Rh analogues is 10^2–10^7. The ordering of associative substitution rates Co << Rh >>> Ir in these clusters exaggerates the trend seen in mononuclear metal complexes.

Introduction

While the mechanism of CO substitution in mononuclear binary carbonyl complexes can occur by both dissociative interchange and dissociative routes, the latter path usually [1] dominates in 18-electron systems. This conforms to the general principle that coordinatively saturated 18-electron complexes react via 16-electron intermediates. In the $M(CO)_6$ triad (M = Cr, Mo, W) the dissociation rate maximizes for M = Mo, which reacts by a factor of 10 and 2000 faster than M = Cr and W, respectively [2]. Phosphite exchange by cyclohexyl isocyanide in $M[P(OEt)_3]_4$ (M = Ni, Pd, Pt) and CO exchange by PPh_3 in $CpM(CO)_2$ (M = Co, Rh, Ir) exhibit similar trends [3] with the relative reactivity orderings Ni(1) <<< Pd(1.8 $\times 10^9$) >> Pt(3×10^4) and Co(1) < Rh(10) > Ir(0.5). The phosphite exchange reactions proceed [3a] by a dissociative mechanism whereas the CO substitution in $CpM(CO)_2$ occurs [3b] by an associative mechanism. Enhanced reactivity for the second row transition metal seems to be a general trend for mononuclear complexes [3c].

Mechanistic paths for reactions of metal carbonyl clusters are by comparison less well defined. Although $M_2(CO)_{10}$ complexes (M = Mn or Re) are now known [4] to substitute by CO dissociative routes, $Mn_2(CO)_8(PPh_3)_2$ may react by Mn–Mn bond cleavage [5], and certain reactions of $Co_2(CO)_8$ appear to involve radical chain pathways, which arise from homolytic Co–Co bond cleavage [6]. For polynuclear cluster complexes substitution and fragmentation processes frequently compete. Substitution reactions that maintain cluster nuclearity may proceed by both associative and dissociative paths. For example, $Fe_3(CO)_{12}$ undergoes substitution and fragmentation reactions with little dependence of the rate on the entering ligand [7]. Therefore, a CO dissociative interchange mechanism has been proposed. Substitution of 3 COs in $Ru_3(CO)_{12}$ occurs in rapid succession [7c, 8] and the observed rate law suggests the presence of both dissociative and dissociative interchange mechanisms, as found for $Cr(CO)_6$ and $Mo(CO)_6$. Substitution of 3COs in $Os_3(CO)_{12}$ by trivalent phosphorus donor ligands occurs by a dissociative mechanism [7a, 9]. Fragmentation, however, appears to involve nucleophilic attack. An alternative mechanism has been proposed [10] to explain the reactions of these clusters, which involves heterolytic cleavage of a metal–metal bond to yield $^+M(CO)_4M(CO)_4M(CO)_4^-$ as an intermediate. In contrast to mononuclear systems the CO dissociation rates of $M_3(CO)_{12}$ clusters follow the order [9] Fe > Ru > Os.

Mechanistic data for the tetranuclear $M_4(CO)_{12}$ clusters (M = Co, Rh, Ir) is available only for $Ir_4(CO)_{12}$, where CO substitution occurs by a two term rate law with a dominant second order process for phosphorus and carbon nucleophiles [11–14].

*Authors to whom correspondence should be addressed.

0020-1693/88/$3.50

Substitution in $Ir_4(CO)_{11-z}L_z$ ($z = 1-3$) occurs primarily by a dissociative route [11, 15–17], when the entering ligand is a phosphorus donor. The mechanism of CO substitution in $Co_4(CO)_{12}$ and $Rh_4(CO)_{12}$ is less well understood. Exchange of CO in $Co_4(CO)_{12}$ with ^{13}CO and ^{14}CO proceeds by a dissociative route, while fragmentation to $Co_2(CO)_8$ (at high temperature and high CO pressure) follows a rate law with first and second order terms in CO [18–22]. In contrast, the reaction between $Co_4(CO)_{12}$ and other ligands L to yield $Co_4(CO)_{11}L$ was too fast to measure, which suggests an associative mechanism [20]. Carbonyl substitution in $Rh_4(CO)_{12}$ occurs so rapidly that only a lower limit could be set on the rate of CO substitution [23]. Since the prototypical $M_4(CO)_{12}$ clusters are important for understanding the mechanism of substitution in clusters we have examined the kinetics of CO substitution in $Co_4(CO)_{12}$ and $Rh_4(CO)_{12}$ using stopped flow methods.

Experimental

Materials

All manipulations were carried out under a prepurified and dried N_2 atmosphere using standard inert atmosphere techniques [24], unless otherwise stated. Dichloromethane was distilled from phosphorus pentoxide. Hexane and pentane were washed with sulfuric acid, predried over sodium hydroxide, and distilled from sodium/benzophenone. Chlorobenzene was washed with H_2SO_4, saturated aqueous sodium bicarbonate, and water; it was then predried over calcium chloride and distilled from P_2O_5. Toluene was distilled from melted sodium. The deuterated toluene solvent was stored over melted sodium, degassed, and vacuum distilled into the reaction vessel.

Triphenylphosphine (PPh_3) was purchased (Strem) and recrystallized from ethanol. ^{13}C labelled carbon monoxide (99%) was purchased (Monsanto). Rhodium trichloride trihydrate was obtained on loan (Johnson-Matthey). Dicobaltoctacarbonyl was purchased (Strem) and stored cold under N_2. The $Rh_4(CO)_{12}$ was synthesized by a literature procedure [25].

Instrumentation

All NMR spectra were recorded with a Varian XLA-400 spectrometer. Chemical shifts are referenced to 85% H_3PO_4 (external reference) for ^{31}P NMR and to TMS for ^{13}C NMR. Positive shifts are downfield. Infrared spectra were recorded on either a Perkin-Elmer Model 283 spectrophotometer or a Nicolet 170-FX Fourier Transform spectrometer. The variable temperature IR cell (SPECAC model P/N 21.000) was equipped with a 0.5 mm path length cell, CaF_2 cell windows, AgCl outer jacket windows, and copper–constantan thermocouple. The stopped flow apparatus was a modified Applied Photophysics (London) Model 1705 instrument with a 2 cm path length quartz cell. The stopped flow spectrometer was interfaced to an Apple II Plus personal computer for data collection. The analog to digital converter, timing board, collection board, and software were purchased from Interactive Microware.

$Co_4(CO)_{12}$

This cluster was synthesized according to modified literature methods [26]. A quantity of $Co_2(CO)_8$ (<10 g) was dissolved in toluene, the solution filtered to remove impurities, heated to 85 °C for 90 min, and to 95 °C for 2 h. The solution was cooled overnight and black crystals formed. These were filtered, dissolved in CH_2Cl_2, and column chromatographed using silica gel (60–200 mesh) as solid support and CH_2Cl_2 as eluent. The solution collected was concentrated and cooled for several days to yield black crystals, whose solution IR spectra matched those reported in the literature [27].

Kinetics Techniques

Substitution reactions that occurred at a rate too fast to monitor by IR or UV–Vis absorption spectroscopy were followed either by use of stopped flow spectrophotometry or by use of a variable temperature IR cell. The major obstacle to conducting kinetic studies with the VT-IR cell is that known volumes of the cluster and ligand solutions must be mixed at low temperature outside the cell and the reaction solution delivered into the VT-IR cell at low temperature. A vacuum jacketed low temperature (LT) syringe proved successful. The VT-IR cell is used with the FT-IR spectrometer operating in single beam mode. A sample of ligand solution at the exact concentration as used during the kinetic reaction was injected into the IR cell. The temperature is allowed to equilibrate and a background spectrum obtained and stored. The cell is cleaned and kept at the desired temperature (N_2 gas flush). Two more slush baths are prepared, one to cool the synringe and one to cool the reagents. These two baths should be 5–10 °C below the VT-IR cell reaction temperature. One problem with the LT syringe concerns cooling the needle, as this part of the syringe is not directly cooled by the slush bath. This problem can be overcome by making the needle as short as possible and by having the reagents and syringe at temperatures slightly below the VT-IR cell reaction temperature so any warming as the solutions pass through the needle only brings the temperature up to reaction temperature, and not above. The flasks in which the reagents are mixed must be small (<5 ml volume) to accommodate the short syringe needle. Care must also be taken to pass dry N_2 gas through

the syringe and over the needle when at temperatures below the dew point of H_2O.

A specified concentration of ligand is added to one flask as a 1.0 ml volume. A second flask is charged with 3.0 ml of a 2.0×10^{-3} M solution of metal complex. These solutions are allowed to equilibrate to the slush bath temperature (5–10 degrees below reaction temperature). The LT syringe is then cooled by adding the third slush bath to the batch chamber (N_2 gas must be blown through syringe). With the LT syringe 5–10 degrees below reaction temperature 1.0 ml of the metal complex solution is delivered to the 1.0 ml solution of ligand. The contents of this flask are mixed rapidly and a known volume drawn up into the LT syringe and injected into the VT-IR cell. The VT-IR cell is placed into the FT-IR spectrophotometer and spectra are recorded for kinetic analysis. This technique was used to study the reaction between $Co_4(CO)_{12}$ and PPh_3 (eqn. (1)) at low temperatures.

$$Co_4(CO)_{12} + PPh_3 \longrightarrow Co_4(CO)_{11}(PPh_3) + CO \quad (1)$$

The stopped flow instrument used in these studies employed a visible light spectrophotometer (light source, monochromator, 2 cm path length quartz cell, and photomultiplier tube) and the reaction was monitored at a single wavelength. The stopped flow kinetic technique has been used to obtain data for the reactions between $Co_4(CO)_{12}$ and PPh_3 (eqn. (1)), between $Rh_4(CO)_{12}$ and PPh_3 (eqn. (2)), and between $Rh_4(CO)_{11}(PPh_3)$ and PPh_3 (eqn. (3)).

$$Rh_4(CO)_{12} + PPh_3 \longrightarrow Rh_4(CO)_{11}(PPh_3) + CO \quad (2)$$

$$Rh_4(CO)_{11}(PPh_3) + PPh_3 \longrightarrow Rh_4(CO)_{10}(PPh_3)_2 + CO \quad (3)$$

The theory and technique of stopped flow kinetic methods have been well discussed [28]. The voltage signal trace obtained from the photomultiplier tube was passed to an analog to digital converter and stored as a set of digital readings on an Apple II Plus personal computer. Data collection was controlled by the computer and readings were obtained at specified time intervals triggered from the internal clock of the computer. The dead-time for the stopped flow equipment used in these studies is about 5 ms. Data was analyzed with the program CURFIT (Interactive Microwave, Inc.).

Results

$Co_4(CO)_{12}$

The reaction of eqn. (1) was studied by both stopped flow and low temperature IR techniques. Substitution is known [29] to yield a product substituted in a basal-axial site of the parent C_{3v} $Co_4(CO)_{12}$.

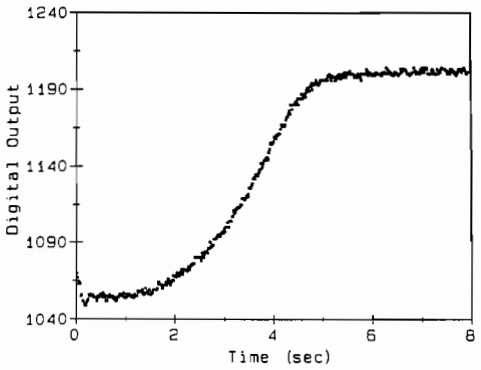

Fig. 1. Stopped flow trace from reaction between $Co_4(CO)_{12}$ and PPh_3 in chlorobenzene solvent at 28 °C.

Figure 1 shows a typical trace for the rise in absorbance at 520 nm (other wavelengths gave similar plots) for the reaction between PPh_3 and $Co_4(CO)_{12}$ in chlorobenzene solvent at 28 °C. The reaction proceeds through an induction period, where little or no reaction takes place, after which the rate accelerates dramatically to completely form product. Thus, rapid substitution in this cluster is not an intrinsic property of $Co_4(CO)_{12}$, but results from some catalytic process.

The time observed for the induction period exceeds or equals the accelerated rate period at low PPh_3 concentrations, and is less than the accelerated rate period at high PPh_3 concentrations. A 10^2 molar range in the entering ligand concentration was employed in this study. The duration of the induction period and the total reaction time are listed with the PPh_3 molar concentrations in Table I. The length of the induction period and the total reaction time exhibit a nonlinear dependence on ligand concentration. The induction periods varied as the amount of sample used to flush the cell between runs varied. Incomplete flushing of the cell shortened the induction period for the subsequent reaction.

The nonlinear kinetic behavior for the reaction between $Co_4(CO)_{12}$ and PPh_3 in chlorobenzene prompted us to conduct a series of low temperature IR experiments. This was done (i) to measure the rate of disappearance of $Co_4(CO)_{12}$ compared to the rate of appearance of $Co_4(CO)_{11}(PPh_3)$, and (ii) to observe any intermediates or by-products formed during the course of reaction. A 1.0×10^{-3} M concentration of the cobalt carbonyl cluster was used in the low temperature IR experiments. Pseudo-first order conditions (25 fold or greater excess of PPh_3) were employed to obtain the kinetic data. The rate data obtained at −43 °C were determined for a greater than ten-fold ligand concentration range (~40- to ~1000-fold excess PPh_3). At −20 °C, a 25- and a 50-fold excess of ligand was used. The first spectrum of any individual kinetic run was obtained within 5 min of mixing the reagents. The substitution

TABLE I. Stopped Flow Data for the Reaction Between $Co_4(CO)_{12}$ and PPh_3 at 28 °C in Chlorobenzene Solvent

$[PPh_3]$ (M)	Induction period (s)	Reaction time (s)	k_{obs} (s^{-1})	Range of k_{obs}	No. of determinations
7.45×10^{-4}	12–15	25–31	0.45	0.39–0.46	3
2.24×10^{-3}	5.0–8.5	12–16	0.73	0.59–0.85	9
7.45×10^{-3}	2.3–3.1	5.5–7.5	1.6	1.3–2.0	12
7.45×10^{-2}	1.4–2.4	4.5–6.5	1.8	1.3–2.2	8

$[Co_4(CO)_{12}] = 1.78 \times 10^{-5}$ M.

reaction (eqn. (1)) appears straightforward and the observation of isosbestic points in the composite spectral diagram of the reaction implies that $Co_4(CO)_{12}$ and $Co_4(CO)_{11}(PPh_3)$ are the only metal carbonyl complexes changing concentration in solution. The decrease in the concentration of $Co_4(CO)_{12}$ was monitored by noting the change in absorbance at 2064 cm^{-1} and the increase in $Co_4(CO)_{11}(PPh_3)$ concentration was monitored at 2083 cm^{-1} [19].

The kinetic behavior observed in the low temperature IR experiments resembles that observed in the stopped flow experiments. No significant difference in behavior was observed between the rate of dis appearance of $Co_4(CO)_{12}$ and the rate of formation of $Co_4(CO)_{11}(PPh_3)$. At −43 °C, over the PPh_3 concentration range studied, the total time of reaction was greater than 10 h. The induction period was observed to be less than the accelerated rate period at all PPh_3 concentrations employed, and there is little correlation between ligand concentration and length of induction period. This contrasts with stopped flow experiments. The duration of the induction period was always 2 h or less at −43 °C. Rates of reaction were zero (within experimental error) during this period.

Although the kinetic behavior was similar for both formation of $Co_4(CO)_{11}(PPh_3)$ and loss of $Co_4(CO)_{12}$, a low temperature ^{13}C NMR (400 MHz) experiment was conducted to further probe the possibility of intermediates or by-products appearing during the reaction. A chlorobenzene/d_8-toluene solution of ^{13}CO enriched $Co_4(CO)_{12}$ was prepared in an NMR tube. A solution of PPh_3 (9 equivalents) was added to the cooled (< −20 °C) $Co_4(CO)_{12}$ solution in the NMR tube and the reaction was monitored at −45 °C. The only species observed were $Co_4(CO)_{12}$ and $Co_4(CO)_{11}(PPh_3)$. After complete formation of $Co_4(CO)_{11}(PPh_3)$ further spectral changes were observed to occur in the IR spectrum and a new absorbance at 2063 cm^{-1} was noted. This process was not amenable to a kinetics study.

$Rh_4(CO)_{12}$

Addition of one or two equivalents of PPh_3 to a chlorobenzene solution of $Rh_4(CO)_{12}$ yields $Rh_4(CO)_{11}(PPh_3)$ and $Rh_4(CO)_{10}(PPh_3)_2$, which were identified by comparison of their infrared spectra to literature spectra [30] determined in CH_2Cl_2. The similarity between the IR spectra of $Rh_4(CO)_{11}(PPh_3)$ and the cobalt analogue [19, 30] suggests that the rhodium cluster also binds PPh_3 in a basal-axial site. In $Rh_4(CO)_{10}(PPh_3)_2$, crystallographic studies [31] show axial and radial substitution on two basal rhodium atoms. A low temperature IR investigation revealed that a 2.0×10^{-3} M solution of $Rh_4(CO)_{12}$ will react with a twenty-fold excess of PPh_3 at −40 °C. An IR spectrum obtained within 5 min of mixing shows only carbonyl stretching absorptions for $Rh_4(CO)_{10}(PPh_3)_2$. To determine the kinetic parameters for the reaction between $Rh_4(CO)_{12}$ and PPh_3, a stopped flow study was performed. Reactions were monitored at several wavelengths between 360 nm and 450 nm; the rate was independent of the wavelength used to monitor the reaction. At low concentrations of PPh_3, the stepwise substitution of CO on $Rh_4(CO)_{12}$ to first form $Rh_4(CO)_{11}(PPh_3)$ and then $Rh_4(CO)_{10}(PPh_3)_2$ is apparent in the stopped flow trace (Fig. 2). By adjusting the observation wavelength, a larger absorbance change can be observed for the first or second substitution depending on which rate one wants to measure.

Rate data have been obtained for the reactions of eqns. (2) and (3) at 28 °C in chlorobenzene solvent. Ligand concentrations from 5.00×10^{-4} to 7.55×10^{-3} M were used to study the initial substitu-

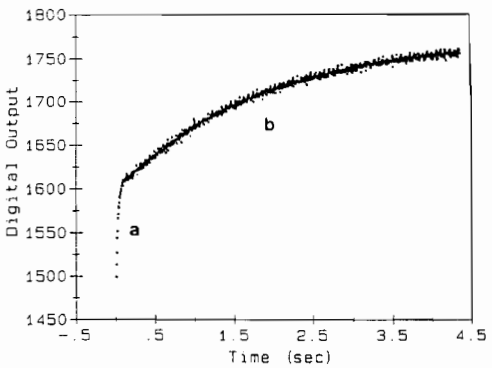

Fig. 2. Stopped flow trace (monitored at 450 nm) from the stepwise substitution reactions ((a) and (b)) of $Rh_4(CO)_{12}$ with PPh_3 in chlorobenzene solvent at 28 °C.

TABLE II. Stopped Flow Rate Data (k_{obs} in s^{-1}) for CO Substitution by PPh_3 in $Rh_4(CO)_{12}$ at 28 °C in Chlorobenzene Solvent

	$[PPh_3]$ (M)		
	5.00×10^{-4}	2.50×10^{-3}	7.55×10^{-3}
	33.2	98.6	344
	38.2	84.8	284
	40.7	122	204
	39.6	75.8	177
	41.5	116	232
	39.3	122	
	34.9	88.2	
	40.3		
avg. k_{obs} [a] =	38.5 (±2.9) s^{-1}	101 (±19) s^{-1}	248 (±67) s^{-1}
k_1 (avg.)[b] =	25.1 (±2.2) s^{-1}		
k_2 (avg.)[b] =	2.96 (±0.05) $\times 10^4$ M^{-1} s^{-1}		
k_1 (all)[c] =	24.9 (±10.9) s^{-1}		
k_2 (all)[c] =	2.97 (±0.27) $\times 10^4$ M^{-1} s^{-1}		

$[Rh_4(CO)_{12}] = 2.50 \times 10^{-5}$ M. [a]Number in parentheses represents one standard deviation on the mean. [b]Value obtained from linear least-squares analysis of the average (avg.) k_{obs} *vs.* $[PPh_3]$ plot. Numbers in parentheses represent one standard deviation. [c]Value obtained from linear least-squares analysis of k_{obs} *vs.* $[PPh_3]$ plot using all values. Number in parentheses represents one σ.

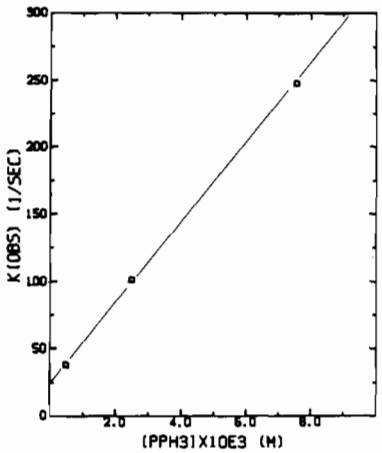

Fig. 3. Plot of k_{obs} (s^{-1}) *vs.* $[PPh_3]$ for the reaction between $Rh_4(CO)_{12}$ and PPh_3 in chlorobenzene solvent at 28 °C.

tion on $Rh_4(CO)_{12}$ (eqn. (2)). At PPh_3 concentrations above 7.55×10^{-3} M and an initial $Rh_4(CO)_{12}$ concentration of 2.50×10^{-5} M, the reaction occurs within the dead-time of the instrument (~5 ms). At a low concentration of PPh_3, the precision of the k_{obs} values is high, but as the rate limits of the instrument are approached the scatter in the data increased (Table II). Figure 3 shows a plot of k_{obs} *versus* $[PPh_3]$, which obeys a two term rate law (eqn. (4)). The ligand independent rate constant (k_1) was about 25 s^{-1} and the ligand dependent rate constant (k_2) was about 30 000 M^{-1} s^{-1} at 28 °C in C_6H_5Cl.

$$\frac{-d[Rh_4(CO)_{12}]}{dt} = (k_1 + k_2[PPh_3])[Rh_4(CO)_{12}] \quad (4)$$

Kinetic data for the formation of $Rh_4(CO)_{10}(PPh_3)_2$ from $Rh_4(CO)_{11}(PPh_3)$ and excess PPh_3 (eqn. (3)) are listed in Table III. Pseudo-first order plots were linear, which show a first order contribution of the $Rh_4(CO)_{11}(PPh_3)$ concentration to the rate law. Additionally, plots of k_{obs} *versus* PPh_3 concentration (Fig. 4) show the rate law may be two termed (eqn. (5)), as that governing the formation of $Rh_4(CO)_{11}(PPh_3)$ (eqn. (4)).

$$\frac{-d[Rh_4(CO)_{11}(PPh_3)]}{dt} = (k_1 + k_2[PPh_3])[Rh_4(CO)_{11}(PPh_3)] \quad (5)$$

The ligand independent rate constant of 1.5×10^{-1} s^{-1} at 28 °C, however, borders on being statistically significant because of the scatter in data points and the extrapolation to zero concentration to obtain its value.

The exchange reaction of eqn. (6) was studied to see whether it affects the kinetics. Addition of $Rh_4(CO)_{12}$ to a chlorobenzene solution of $Rh_4(CO)_{10}(PPh_3)_2$ results in the formation of $Rh_4(CO)_{11}(PPh_3)$ after several hours at room temperature, a reaction too slow to be involved in the rapid reaction between $Rh_4(CO)_{12}$ and PPh_3. These results confirm other findings [31]. After standing in solution, further spectral changes occurred after formation of $Rh_4(CO)_{11}(PPh_3)$ in the reaction mixture (eqn. (6)), which may result from isomerization, as reported previously [31], but this was not investigated.

TABLE III. Stopped Flow Rate Data (k_{obs} in s^{-1}) for CO Substitution by PPh_3 in $Rh_4(CO)_{11}(PPh_3)$ at 28 °C in Chlorobenzene Solvent

	[PPh_3] (M)			
	5.00×10^{-4}	2.50×10^{-3}	7.55×10^{-3}	2.52×10^{-2}
	0.462	1.675	5.28	16.40
	0.483	1.688	5.79	16.02
	0.399	1.729	4.71	16.26
	0.488	1.762	4.68	16.97
	0.516	1.818	5.05	17.33
	0.532	1.833	4.72	17.26
	0.521	1.901	4.80	15.84
			5.52	16.88
			5.34	
avg. k_{obs}[a]	0.486 (±0.045) s^{-1}	1.772 (±0.083)	5.10 (±0.40)	16.62 (±0.57)
k_1 (avg.)[b] =	0.154 (±0.010) s^{-1}			
k_2 (avg.)[b] =	6.54 (±0.01) $\times 10^2$ M^{-1} s^{-1}			
k_1 (all)[c] =	0.154 (±0.089) s^{-1}			
k_2 (all)[c] =	6.54 (±0.07) $\times 10^2$ M^{-1} s^{-1}			

[$Rh_4(CO)_{11}(PPh_3)$] = 2.50×10^{-5} M. [a]Number in parentheses represent one standard deviation. [b]Value obtained from linear least-squares analysis of the average (avg.) k_{obs} *vs.* [PPh_3] plot. Number in parentheses represents one σ. [c]Value obtained from linear least-squares analysis of k_{obs} *vs.* [PPh_3] plot using all values. Number in parentheses represents one σ.

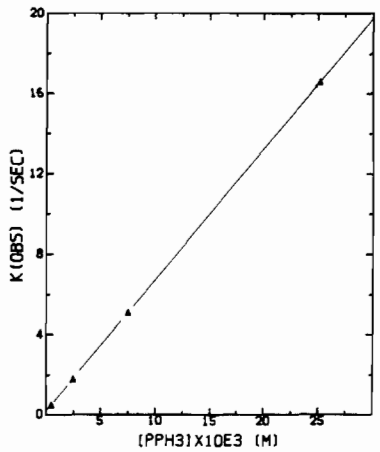

Fig. 4. Plot of k_{obs} (s^{-1}) *vs.* [PPh_3] for the reaction between $Rh_4(CO)_{11}(PPh_3)$ and PPh_3 in chlorobenzene solvent at 28 °C.

$$Rh_4(CO)_{12} + Rh_4(CO)_{10}(PPh_3)_2 \longrightarrow 2Rh_4(CO)_{11}(PPh_3) \quad (6)$$

Discussion

The rapid formation of $Co_4(CO)_{11}(PPh_3)$ at room temperature in a solution of $Co_4(CO)_{12}$ and PPh_3 has been shown to proceed too fast to be governed by a CO dissociative path [19]. This reaction is reported to be unaffected by addition of the radical trap 2,6-di-t-butylphenol [20]. Good evidence has been presented that the reaction does not proceed via a cluster fragmentation–reformation mechanism [32]. Reactions between $Co_4(CO)_{12}$ and a variety of phosphorus donor ligands proceed rapidly to yield $Co_4(CO)_{11}L$ in the absence of light. These reactions have been suggested to proceed by an associative or interchange mechanism, perhaps involving metal–metal bond cleavage [20, 32]. Our studies of the reaction between $Co_4(CO)_{12}$ and PPh_3 to form $Co_4(CO)_{11}(PPh_3)$ in chlorobenzene solvent show that this rapid reaction does not follow simple associative or interchange mechanisms.

The reaction between $Co_4(CO)_{12}$ and PPh_3 to afford $Co_4(CO)_{11}(PPh_3)$ proceeds in two stages. The initial stage involves little or no reaction, followed by a period where the reaction rate accelerates to completely form the product. This latter period appears to be autocatalytic. Both loss of $Co_4(CO)_{12}$ and formation of $Co_4(CO)_{11}(PPh_3)$ follow this kinetic behavior. No detectable reaction occurs during the induction period. The CO dissociation rate constant determined from CO exchange reactions of $Co_4(CO)_{12}$ [20] is about 2.3×10^{-5} s^{-1} at 28 °C. This represents a half-life of reaction of 3×10^4 s, but the longest induction period we observed at this temperature was 15 s. At −43 °C, the CO dissociative rate constant is about 4.5×10^{-11} s^{-1}, corresponding to a half-life of 500 years! The induction period at this temperature was always less than 2 h. Considering the extent of reaction possible, observation of the CO dissociative reaction during the induction period is not expected.

TABLE IV. Comparison of k_1 Values for CO Substitution in $M_4(CO)_{12}$ and $M_4(CO)_{11}(PPh_3)$ (M = Co, Rh, Ir) Clusters at 28 °C

Reactant	Ligand	Solvent	k_1 (s^{-1})	Rel k_1	Reference
$Co_4(CO)_{12}$	^{13}CO	C_6H_{14}	2.3×10^{-5} [a]	1	19
$Rh_4(CO)_{12}$	PPh_3	C_6H_5Cl	~25	10^6	this work
$Ir_4(CO)_{12}$	$AsPh_3$	C_6H_5Cl	$<8 \times 10^{-10}$ [b]	$<4 \times 10^{-5}$	13
$Co_4(CO)_{11}(P(OMe)_3)$	PPh_3	C_6H_{14}	1.4×10^{-5} [b]	1	20
$Co_4(CO)_{11}(P(OEt)_3)$	^{13}CO	C_7H_{16}	1.7×10^{-5} [a]	1	19
$Co_4(CO)_{11}(PPh_3)$	PPh_3	C_7H_{16}	3×10^{-4} [c]	20	
$Rh_4(CO)_{11}(PPh_3)$	PPh_3	C_6H_5Cl	$\sim 1.5 \times 10^{-1}$	10^4	this work
$Ir_4(CO)_{11}(PPh_3)$	PPh_3	C_6H_5Cl	6×10^{-8} [b]	4×10^{-3}	11

[a]Estimate at 28 °C from k_1 activation parameters. [b]Estimate at 28 °C from k_{obs} activation parameters of predominate k_1 reaction. [c]k_{obs} at 20 °C, rate law unknown.

A possible mechanism for the catalytic process could involve redox catalysis. Recent results [33] have shown $Co_4(CO)_9[HC(PPh_2)_3]$ is subject to electrocatalyzed substitution reactions. Thus, the radical anion $Co_4(CO)_9[HC(PPh_2)_3]^-$, generated either chemically or electrochemically, undergoes CO substitution much more rapidly than neutral $Co_4(CO)_9[HC(PPh_2)_3]$. These reactions were suggested to proceed via a CO dissociative pathway. The initial electron transfer in our system may involve a phosphine substituted derivative of $Co_4(CO)_{12}$. The induction period may allow formation of a polysubstituted cluster because the rate of reaction on the neutral clusters increases [34, 35] during the stepwise formation of $Co_4(CO)_8(PPh_3)_4$ from $Co_4(CO)_{11}(PPh_3)$. The possibility of oxidative catalysis from traces of O_2 cannot be excluded.

A linear relationship was shown to exist between the degree of substitution (n) and the oxidation potential of $Co_4(CO)_{12-n}L_n$ clusters [33, 36, 37]. Reduction becomes more difficult and oxidation becomes easier as the degree of substitution by phosphine increases on these clusters [33, 36–38]*. Thus the higher substituted $Co_4(CO)_{12}$ derivatives, or fragments derived from them, may act as reductants toward $Co_4(CO)_{12}$. On the cyclic voltammetry time scale the $Co_4(CO)_{12}/Co_4(CO)_{12}^-$ couple exhibits chemical reversibility in DCE solvent at −0.303 V *versus* SCE [33, 37]. This low reduction potential in comparison to $Rh_4(CO)_{12}$ or $Ir_4(CO)_{12}$ [38] helps explain why only $Co_4(CO)_{12}$ exhibits unusual kinetic behavior. Attempts to apply electrochemical techniques to probe for redox catalysis were unsuccessful because the normal thermal catalytic process interfered. Radical behavior may also be responsible for the reported [20, 39] observation that $Co_4(CO)_{11}(P(OMe)_3)$ reacts with $P(OMe)_3$ via a ligand dependent process but the rates of reaction are CO inhibited.

The cluster $Rh_4(CO)_{12}$ reacts with PPh_3 in chlorobenzene solutions at 28 °C under pseudo-first order conditions to yield, in consecutive reactions, $Rh_4(CO)_{11}(PPh_3)$ and $Rh_4(CO)_{10}(PPh_3)_2$. Substitution to form $Rh_4(CO)_{11}(PPh_3)$ occurs faster than the following reaction to form $Rh_4(CO)_{10}(PPh_3)_2$. Both reactions obey two term rate laws (eqns. (4) and (5), respectively) and both the ligand independent (k_1) and ligand dependent (k_2) rate constants are smaller for formation of $Rh_4(CO)_{10}(PPh_3)_2$ from $Rh_4(CO)_{11}(PPh_3)$ than for formation of $Rh_4(CO)_{11}(PPh_3)$ from $Rh_4(CO)_{12}$. Because of the high reactivity of $Rh_4(CO)_{12}$ and its phosphine derivatives with CO, the ligand independent pathway could not be tested for CO inhibition. Addition of excess CO causes cluster fragmentation to occur [32, 40].

With these new observations for $Co_4(CO)_{12}$ and $Rh_4(CO)_{12}$ one can make reactivity comparisons among the $M_4(CO)_{12}$ cluster series. Table IV lists the estimated k_1 values for $M_4(CO)_{12}$ and $M_4(CO)_{11}(PPh_3)$ derivatives adjusted to 28 °C. It has been shown that the k_1 term, attributed to CO dissociation, depends on the specific L in $Co_4(CO)_{11}L$ and $Ir_4(CO)_{11}L$ clusters. Therefore $L = PPh_3$ is chosen to compare these clusters. Unfortunately no accurate k_1 value is known for $Co_4(CO)_{11}(PPh_3)$, so values from reactions of other $Co_4(CO)_{11}L$ species must be used as estimates. Our study of the reactions of $Co_4(CO)_{12}$ with PPh_3 in C_6H_5Cl solvent yields an upper limit for k_2.

In both $M_4(CO)_{12}$ and $M_4(CO)_{11}(PPh_3)$ clusters the relative values of k_1 for rhodium significantly exceed those for the cobalt and iridium, and the rate for cobalt exceeds that for iridium. Indeed, the k_1 value for $Rh_4(CO)_{12}$ exceeds that for iridium by 10^{10} and that for cobalt by 10^6 (Table IV). In $M_4(CO)_{11}(PPh_3)$, this difference decreases somewhat, as the k_1 value for rhodium is 10^6 greater than for iridium and at most 10^4 greater than for cobalt (Table IV). Hence, rhodium exhibits a much greater lability

*The reduction potentials for $Co_4(CO)_{11}(PPh_3)$ are not experimental values but estimates based on the linear relationship between degree of substitution and redox couple potential (−200 mV per n).

toward CO dissociation (assuming the k_1 term represents this pathway) than either cobalt or iridium. This trend in dissociative rates Co << Rh >>> Ir parallels that found for reactions of $M(CO)_6$ complexes discussed in 'Introduction'; however, the magnitude of the effect in the clusters is greater.

The observation [11] of a drastic increase in the k_1 term for CO substitution in $Ir_4(CO)_{12-n}(PPh_3)_n$ clusters, as n increases from zero to two, provided an impetus to further studies on $M_4(CO)_{12}$ clusters. It was believed that $M_4(CO)_{12}$ clusters could show a cooperativity between metal centers in their reactivity, *i.e.* a cluster effect. Later, studies on cobalt derivatives [19, 20, 34, 39, 41] revealed they behaved differently than iridium clusters as consecutive substitution of CO by phosphorus donor ligands had little effect on the k_1 term. Our studies for rhodium show that the behavior of the k_1 term differs from cobalt or iridium because the stepwise substitution of CO by phosphine decreases the k_1 term. The relative values of k_1, estimated at 28 °C from reported activation parameters and our data (Table IV), for stepwise substitution of CO on cobalt [19], rhodium, and iridium [15] clusters are shown in eqns. (7)–(9).

$$Co_4(CO)_{12} \xrightarrow{1.0} Co_4(CO)_{11}[P(OMe)_3] \xrightarrow{0.6} Co_4(CO)_{10}[P(OMe)_3](PPh_3) \quad (7)$$

$$Rh_4(CO)_{12} \xrightarrow{1.0} Rh_4(CO)_{11}(PPh_3) \xrightarrow{0.006} Rh_4(CO)_{10}(PPh_3)_2 \quad (8)$$

$$Ir_4(CO)_{12} \xrightarrow{1.0} Ir_4(CO)_{11}(PPh_3) \xrightarrow{>60} Ir_4(CO)_{10}(PPh_3)_2 \quad (9)$$

Thus, cobalt shows a slight effect, iridium shows enhanced reactivity, and rhodium shows reduced reactivity of the k_1 path as the degree of substitution increases.

Ligand dependent rate constants, k_2, for CO substitution reactions on $M_4(CO)_{12}$ clusters (M = Co, Rh, Ir), adjusted to 28 °C using reported activation parameters, are compared in Table V. The scope of this comparison and the required estimate of certain k_2 values lessen the quantitative accuracy of comparison, but the trends are unambiguous. We could not obtain data for a ligand dependent term from room temperature UV–Vis stopped flow and low temperature IR kinetic experiments involving reactions of $Co_4(CO)_{12}$ with PPh_3. An upper limit on k_2 can be set with the assumption that, at most, 10% reaction occurred during the induction period. For substitution reactions of $M_4(CO)_{12}$ with PPh_3, the rhodium associative rate constant is 10^{11} greater than for iridium. The reactions of $M_4(CO)_{11}(PPh_3)$ with PPh_3 are similar in that rhodium reacts 10^7 faster than iridium and at least 10^5 faster than the rate for cobalt. These relative values of k_2 parallel trends in relative values of k_1. Thus, for $M_4(CO)_{12}$, relative k_1 values of 10^4:10^{10}:1 (Co:Rh:Ir) compare well with relative k_2 values of $<10^7$:10^{11}:1 (Co:Rh:Ir). For $M_4(CO)_{11}(PPh_3)$, relative k_1 values of 10^2:10^6:1 (Co:Rh:Ir) compare with relative k_2 values of 10^2:10^7:1 (Co:Rh:Ir). The presence of a catalytic path for substitution in $Co_4(CO)_{12}$ and not for Rh or Ir analogues is attributed to the much greater ease with which the Co species is reduced [33, 36]. These results should be contrasted to the reactivity of $M_3(CO)_{12}$ clusters where the reactivity toward CO dissociation is Fe > Ru > Os [7] with the rates at 298 K in the ratio 10^5:10^4:1.

The rate of associative reaction, k_2, decreases as the degree of substitution by PPh_3 increases on $Rh_4(CO)_{12}$ clusters, similar to the k_1 term. This contrasts with the larger observed k_2 value for $Ir_4(CO)_{11}(PPh_3)$ than $Ir_4(CO)_{12}$ at 89 °C (Table V). The relative change in k_2 on phosphine substitution

TABLE V. Comparison of k_2 Values for CO Substitution in $M_4(CO)_{12}$ and $M_4(CO)_{11}(PPh_3)$ (M = Co, Rh, Ir) Clusters at 28 °C

Cluster	Ligand	Solvent	k_2 (M^{-1} s^{-1})	Rel k_2	Reference
$Co_4(CO)_{12}$	PPh_3	C_6H_5Cl	<3[a]	$<10^7$	this work
$Rh_4(CO)_{12}$	PPh_3	C_6H_5Cl	3.0×10^4	10^{11}	this work
$Ir_4(CO)_{12}$	PPh_3	C_6H_5Cl	1.6×10^{-7} [b]	1	13
$Ir_4(CO)_{12}$	PPh_3	C_6H_5Cl	9.1×10^{-5} [c]		13
$Co_4(CO)_{11}(PPh_3)$	PPh_3	C_7H_{16}	$\leq 5 \times 10^{-3}$ [d]	10^2	34
$Rh_4(CO)_{11}(PPh_3)$	PPh_3	C_6H_5Cl	6.5×10^2	10^7	this work
$Ir_4(CO)_{11}(PPh_3)$	PPh_3	$C_{10}H_{22}$	5×10^{-5} [e]	1	15
$Ir_4(CO)_{11}(PPh_3)$	PPh_3	$C_{10}H_{22}$	4.6×10^{-3} [c]		15

[a]Limit derived by assuming at most 10% undetected reaction occurred during the induction period. [b]Estimate at 28 °C from k_{obs} activation parameters of the predominantly k_2 reaction. [c]At 89 °C. [d]At 20 °C [PPh_3] = 6×10^{-2} M and $k_{obs} = 3 \times 10^{-4}$ s^{-1}. [e]This value is roughly estimated by assuming a $\Delta H^{\dagger}$ of 15 kcal/mole, typical of associative reactions, and calculating the k_2 value at 28 °C knowing the reported k_2 value at 89.5 °C [15]. Changing $\Delta H^{\dagger}$ from 10 kcal/mole to 20 kcal/mole alters the k_2 estimate at 28 °C from 2×10^{-4} M^{-1} s^{-1} to 1×10^{-5} M^{-1} s^{-1}.

in $Rh_4(CO)_{12}$ and $Ir_4(CO)_{12}$ is illustrated in eqns. (10) and (11), respectively.

$$Rh_4(CO)_{12} \xrightarrow[C_6H_5Cl]{1.0} Rh_4(CO)_{11}(PPh_3) \xrightarrow[C_6H_5Cl]{0.02} Rh_4(CO)_{10}(PPh_3)_2 \quad (10)$$

$$Ir_4(CO)_{12} \xrightarrow[C_6H_5Cl]{1.0} Ir_4(CO)_{11}(PPh_3) \xrightarrow[C_{10}H_{22}]{50} Ir_4(CO)_{10}(PPh_3)_2 \quad (11)$$

It is interesting to compare the predominant term of the rate law for the substitution reactions (eqns. (12) and (13)). For the reaction of eqn. (12), with M = Co and L = PPh_3, the rate law is unknown and not simple, although a CO dissociative path has been measured when L = ^{13}CO. The same reaction when M = Rh and L = PPh_3 obeys a two term rate law, and when M = Ir, a primarily ligand dependent rate law is found. The reaction illustrated in eqn. (13) follows a two term rate law when M = Co. When M = Rh and L = PPh_3, a two term rate law is observed (similar to, but slower than, $Rh_4(CO)_{12}$), and when M = Ir a CO dissociative rate law predominates (a switch from $Ir_4(CO)_{12}$ because of a drastic increase in the k_1 contribution to the rate law). Rhodium carbonyl clusters are more prone to associative substitution reactions than are either cobalt or iridium carbonyl clusters. More limited data for the $M_3(CO)_{12}$ clusters [7–9] suggest $Ru_3(CO)_{12}$ is considerably more susceptible than $Os_3(CO)_{12}$ toward nucleophilic attack.

$$M_4(CO)_{12} + L \longrightarrow M_4(CO)_{11}L + CO \quad (12)$$

$$M_4(CO)_{11}L + L' \longrightarrow M_4(CO)_{10}LL' + CO \quad (13)$$

Conclusions

We have shown that the rapid substitution of CO by PPh_3 on $Co_4(CO)_{12}$ in chlorobenzene solvent does not take place via an associative or interchange mechanism but may be subject to redox catalysis. Indeed electron transfer catalysis is a well documented mechanism for substitution reactions in mononuclear and polynuclear complexes [42]. Contrary to this, the rapid substitution reactions of $Rh_4(CO)_{12}$ follow pseudo-first order behavior and obey a two term rate law with both ligand dependent and ligand independent terms. Our studies allow for the complete ordering of the k_1 term for $M_4(CO)_{12}$ clusters as Rh > Co > Ir. This ordering is expected when previous studies on mononuclear systems are considered. However when compared to the Fe > Ru > Os ordering of the $M_3(CO)_{12}$ system this is perhaps unexpected.

The only apparent similarity between the kinetic behavior of the $M_3(CO)_{12}$ and $M_4(CO)_{12}$ clusters and their substituted derivatives is an increased susceptibility to attack by nucleophiles for the second row transition metals. If this reactivity trend proves general then it may reflect the operation of two opposing periodic trends Second row transition metals, because of their greater size, should be more susceptible to nucleophilic attack than first row metals. Since second and third row metals have similar sizes, steric effects should be less important in determining their comparative reactivities. First row transition metals have lower energy frontier acceptor orbitals [38] on the metal than the second or third row metals. Thus trends in frontier orbital energies may run counter to steric effects on reactivity. For metal carbonyl clusters the structural changes caused by the decreasing tendency of carbonyl bridging on descending the triad introduces a further complication. Since bridging carbonyls withdraw more electron density than terminal carbonyls [38, 43] this may enhance electrophilicity at the metal core.

Both $M_3(CO)_{12}$ and $M_4(CO)_{12}$ clusters are electron saturated. In both systems the third row metal cluster reacts the slowest and has the highest energy carbonyl fluxional processes. In the $M_3(CO)_{12}$ clusters the Ru and Os derivatives have similar structures in which there are no bridging carbonyls and the Fe derivative has bridging carbonyls. In the $M_4(CO)_{12}$ clusters the Co and Rh derivatives have similar structures in which there are bridging carbonyls, and the Ir derivative has no bridging carbonyls. For any set of $M_3(CO)_{12}$ or $M_4(CO)_{12}$ clusters with equivalent carbonyl configurations it appears that the reactivity trends observed in mononuclear systems are observed in clusters (*i.e.* Ru > Os and Rh > Co). However, when there are structural differences between a set, the cluster with the higher degree of bridging carbonyls can react faster (e.g. Fe > Ru). This might imply that a ground state bridging carbonyl configuration lies closer in energy to the transition state than a nonbridged form. This idea of the importance of the carbonyl configuration and the influence of the carbonyl fluxionality on reactivity needs to be explored in much greater detail for these and other systems.

Acknowledgement

This material is based on work supported by the National Science Foundation (Grants CHE-85-04088 and CHE 85-14366).

References

1 C. A. Tolman, *Chem. Soc. Rev.*, *1*, 337 (1972).
2 (a) J. R. Graham and R. J. Angelici, *Inorg. Chem.*, *6*, 2082 (1967); (b) J. A. S. Howell and P. M. Burkinshaw, *Chem. Rev.*, *83*, 557 (1983).

3 (a) M. Meier, F. Basolo and R. G. Pearson, *Inorg. Chem., 8,* 795 (1969); (b) H. G. Schuster-Woldan and F. Basolo, *J. Am. Chem. Soc., 88,* 1657 (1966); (c) J. D. Atwood, 'Inorganic and Organometallic Reaction Mechanisms', Brooks/Cole, Monterey, Calif., 1985, pp. 108–111.
4 J. D. Atwood, *Inorg. Chem., 20,* 4031 (1981); S. P. Schmidt, W. C. Trogler and F. Basolo, *Inorg. Chem., 21,* 1698 (1982); E. L. Muetterties, R. R. Burch and A. M. Stolzenberg, *Ann. Rev. Phys. Chem., 33,* 89 (1982).
5 A. J. Poë and C. V. Sekhar, *J. Am. Chem. Soc., 107,* 4874 (1985).
6 R. W. Wegman and T. L. Brown, *Organometallics, 1,* 47 (1982); P. F. Barrett, *Can. J. Chem., 52,* 3773 (1974); M. Asbi-Halabi, J. D. Atwood, N. P. Forbes and T. L. Brown, *J. Am. Chem. Soc., 102,* 6248 (1980).
7 (a) A. Shojaie and J. D. Atwood, *Organometallics, 4,* 187 (1985); (b) R. Kumar, *J. Organomet. Chem., 136,* 235 (1977); (c) G. Cetini, O. Gambino, E. Sappa and G. A. Vaglio, *Atti. Acad. Sci. Torino Cl. Sci. Fis. Mat. Nat., 101,* 855 (1966–1967).
8 (a) J. P. Candlin and A. C. Shortland, *J. Organomet. Chem., 16,* 289 (1969); (b) A. J. Poë and M. V. Twigg, *J. Chem. Soc., Dalton Trans.,* 1860 (1974); (c) A. J. Poë and M. V. Twigg, *Inorg. Chem., 13,* 2982 (1974); (d) M. V. Twigg, *Inorg. Chim. Acta, 21,* L7 (1977).
9 A. J. Poë and V. C. Sekhar, *Inorg. Chem., 24,* 4376 (1985).
10 B. F G. Johnson, *Inorg. Chim. Acta 115* L39 (1986).
11 K. J. Karel and J. R. Norton, *J. Am. Chem. Soc 96* 6812 (1974).
12 K. Dahlinger, F. Falcone and A. J. Poë, *Inorg. Chem. 25,* 2654 (1986).
13 D. C. Sonnenberger and J. D. Atwood, *Inorg. Chem. 20,* 3243 (1981).
14 G. F. Stuntz and J. R. Shapley, *J. Organomet. Chem. 213,* 389 (1981).
15 D. C. Sonnenberger and J. D. Atwood, *J. Am. Chem. Soc., 104,* 2113 (1982).
16 D. C. Sonnenberger and J. D. Atwood, *Organometallics, 1,* 694 (1982).
17 D. J. Darensbourg and B. J. Baldwin-Zuschke, *J. Am. Chem. Soc., 104,* 3906 (1982).
18 D. F. Keeley and R. E. Johnson, *J. Inorg. Nucl. Chem., 11,* 33 (1959).
19 D. J. Darensbourg, B. S. Peterson and R. E. Schmidt, Jr., *Organometallics, 1,* 306 (1982).
20 D. J. Darensbourg and M. J. Incorvia, *Inorg. Chem., 19,* 2585 (1980).
21 G. Cetini, I. Gambino, E. Sappa and G. A. Vaglio, *Ric. Sci., 37,* 430 (1967).
22 G. Bor, U. K. Dietler, P. Pino and A. J. Poë, *J. Organomet. Chem., 154,* 301 (1978).
23 J. R. Norton and J. P. Collman, *Inorg. Chem., 12,* 476 (1973).
24 D. F. Shriver, 'The Manipulation of Air Sensitive Compounds', McGraw-Hill, New York, 1969.
25 S. Martinengo, G. Giordano and P. Chini, *Inorg. Synth., 20,* 209 (1980).
26 P. Chini, V. Albano and S. Martinengo, *J. Organomet. Chem., 16,* 471 (1969).
27 K. Noack, *Helv. Chim. Acta, 45,* 1847 (1962).
28 P. Moore, 'Stopped Flow. An Experimental Manual', copyright P. Moore, University of Warwick, Coventry, U.K., 1972, and refs. therein.
29 D. J. Darensbourg and M. J. Incorvia, *Inorg. Chem., 20,* 1911 (1981).
30 R. Whyman, *J. Chem. Soc., Dalton Trans.,* 1375 (1972).
31 B. T. Heaton, L. Longhetti, D. M. P. Mingos, C. E. Briant, P. C. Marshall, B. R. C. Theobald, L. Garlaschelli and U. Sartorelli, *J. Organomet. Chem., 213,* 333 (1981).
32 D. J. Darensbourg and D. J. Zalewski, *Inorg. Chem., 23,* 4382 (1984).
33 D. Rimmelin, P. Lemoine, M. Gross, A. A. Bahsoun and J. A. Osborn, *Nouv. J. Chim., 9,* 181 (1985).
34 R. Huq and A. J. Poë, *J. Organomet. Chem., 226,* 277 (1982).
35 G. Cetini, O. Gambino, R. Rossetti and P. L. Stanghellini, *Inorg. Chem., 7,* 609 (1968).
36 G. F. Holland, D. E. Ellis and W. C. Trogler, *J. Am. Chem. Soc., 108,* 1884 (1986).
37 J. Rimmelin, P. Lemoine, M. Gross and D. de Montauzon, *Nouv. J. Chim., 7,* 453 (1983).
38 G. F. Holland, D. E. Ellis, D. R. Tyler, H. B. Gray and W. C. Trogler, *J. Am. Chem. Soc., 109,* 4276 (1987).
39 D. J. Darensbourg and M. J. Incorvia, *J. Organomet. Chem., 171,* 89 (1979).
40 B. L. Booth, M. J. Else, R. Fields and R. N. Hazeldine, *J. Organomet. Chem., 27,* 119 (1971).
41 D. J. Darensbourg and D. J. Zalewski, *Organometallics, 4,* 92 (1985).
42 J. K. Kochi, *J. Organomet. Chem., 300,* 139 (1986).
43 J. S. Kristoff and D. F. Shriver, *Inorg. Chem., 13,* 499 (1974).